A LETTERS JOURNAL EXPLORING THE FRONTIERS OF PHYSICS

Società Italiana di Fisica

PERSPECTIVE

Motional quantum metrology in a Penning trap

To cite this article: Javier Cerrillo and Daniel Rodríguez 2021 *EPL* **134** 38001

A Letters Journal Exploring the Frontiers of Physics

May 2021

EPL, **134** (2021) 38001
doi: 10.1209/0295-5075/134/38001

www.epljournal.org

Perspective

Motional quantum metrology in a Penning trap

Javier Cerrillo[1(a)] and Daniel Rodríguez[2,3(b)]

[1] *Área de Física Aplicada, Universidad Politécnica de Cartagena - 30202 Cartagena, Spain*
[2] *Departamento de Física Atómica, Molecular y Nuclear, Universidad de Granada - 18071 Granada, Spain*
[3] *Centro de Investigación en Tecnologías de la Información y las Comunicaciones, Universidad de Granada 18071 Granada, Spain*

received 2 June 2021; accepted in final form 8 June 2021
published online 14 July 2021

Abstract – We propose to measure the six motional frequencies of an unbalanced two-ion crystal in a Penning trap using a scheme that has been demonstrated in a quantum-metrology experiment with a single ion in a linear Paul trap. To study the feasibility, we derive the quantum Hamiltonian for the unbalanced crystal formed by a target and a sensor ion ($^{40}Ca^+$), and deduce characteristic coordinates $\xi_{c'}^{\pm}, \xi_z^{\pm}$, and $\xi_m^{\pm}$, associated to the amplitudes of the displacement operator $\alpha_{c'}^{\pm}, \alpha_z^{\pm}$, and $\alpha_m^{\pm}$, respectively, when a dipolar time-varying field is applied. The final state after excitation is read out using rapid adiabatic passage. We also present the status of the 7 tesla open-ring Penning trap where first experiments on the $^{232}Th^+$-$^{40}Ca^+$ crystal, cooled to the ground state, are foreseen in the short-term future. Finally, we underline possible experiments with this unique platform.

Introduction. – Penning traps [1] are used for ultra-accurate determination of motional frequencies (eigenfrequencies) of a stored charged particle or antiparticle [2], from which one obtains its cyclotron frequency as if it moved in a pure magnetic field. The method utilized is based on resonant electronic detection, first reported in 1975 by Wineland and Dehmelt using an ensemble of electrons [3]. It has been pushed to an outstanding performance using a single stored (anti)particle [4,5] or two particles under sufficient separation [6–8]. See, *e.g.*, the recent review in ref. [9] with implications in several fields. However, the mass and charge of the particle to be measured is limited with this technique to a certain range and one of the eigenfrequencies has to be equal to the resonance frequency of the detector circuit, which is fixed, immersed in a liquid helium tank (see, *e.g.*, [10]). The circuit is also used to cool one of the eigenmotions, with a rate that scales with the square of the particle's charge. This is particularly suitable for ions with large electronic charge states [11], that can be generated by charge breeding using an electron beam ion trap (EBIT) [12], although this process is not always possible.

A new ion-trap experimental activity started at the University of Granada in 2012, devoted to the implementation of a novel Penning-trap mass-spectrometry approach, based on using a single laser-cooled sensor $^{40}Ca^+$ ion as detector [13]. It follows the idea described in ref. [14], relying on the interaction between the sensor ion and the ion of interest, stored in physically separated traps, through the oscillating charges both ions induce in a common electrode. One of the prime motivations was to apply this technique for mass measurements on superheavy elements (SHE), for which the existing (destructive) techniques in 2012 [15] were already at the edge of capabilities [16,17]. Although a novel (destructive) technique was developed in 2013 [18], which has rendered practicable the lighter SHE ions, produced at a smaller rate compared to those measured earlier [19], the technique might not be adequate when dealing with heavier SHEs, as this needs a few ions for the measurement. Initially with this motivation, two separate directions have been pursued after the original proposal. On the one hand, quartz resonators for electronic detection (*vs.* superconducting coils) have been developed in collaboration with the division of Michael Block (University of Mainz, Helmholtz Institute Mainz and GSI-Darmstadt) providing the first quartz-based experiment with ions [20], mass measurements [21], and recently introducing the new feature of fast (non-destructive) resonant detection in a Penning trap [22]. On the other hand, simultaneous storage in the same Penning trap of both the sensor and the target

(a) E-mail: javier.cerrillo@upct.es
(b) E-mail: danielrodriguez@ugr.es (corresponding author)

ions is being explored [23], forming an unbalanced ion crystal cooled first to the Doppler limit [24,25] and later to the ground state of motion (in all spatial directions). With $^{40}Ca^{+}$ ion as the sensor, this implementation will allow detection and measurement of single ions (atomic or molecular) in a vast mass range, expanding classical Penning-trap mass spectroscopy into the quantum regime for ultra-sensitive and universal mass/energy metrology. The information encoded in the electronic states of the embedded sensor qubit in the unbalanced two-ion crystal will be used to measure the cyclotron frequency of the target ion. Such crystal in a Penning trap will constitute a novel platform not only for mass spectrometry but also for quantum logic spectroscopy, developed so far for radiofrequency (RF) traps [26,27]. In this publication, relying on existing protocols to cool an ion crystal in a Penning trap [28], we develop a theoretical framework to describe the effect of applying external dipolar fields in terms of the displacement operator for any of the modes of the ion crystal, and explore precision read out by projecting the generated coherent state into the ground state of the crystal using rapid adiabatic passage (RAP) [29,30]. We also present the current status of the facility and underline the potential of using such a platform for precision spectroscopy free of radiofrequency fields. Particularly, we mention the case of $^{232}Th^{+}$ to address later the $^{229m}Th^{+}$ ion [31–33] proposed as nuclear clock. Generally, isotopes that can be produced by laser desorption can be also studied in a similar way. Some practicable example might be $^{139}La^{2+}$, proposed for telecom applications [34] or specific molecular ions for the study of chirality associated to enantiomers (chiral isomers) at the single-ion level [35] in the Penning trap.

Quantum description of an unbalanced two-ion crystal in a Penning trap. – Particles with mass m and electronic charge q are confined in a Penning trap by the superposition of a strong homogeneous magnetic field $\mathbf{B} = B\mathbf{k}$, and an electrostatic field originated from a potential of the form $V = (U/4d_0^2)\cdot\left(2z^2 - x^2 - y^2\right)$, which is formed by a set of electrodes, generally named ring and endcaps [1]. In all configurations, U is the potential difference between the ring electrode and endcaps and d_0 is a characteristic length of the trap, related to its size and geometry. When dealing with a single ion, the motion can be depicted as the superposition of three eigenmotions, one parallel to the magnetic field (axial motion) with frequency

$$\omega_z = \sqrt{\frac{qU}{md_0^2}}, \tag{1}$$

and two in the radial plane with frequencies approximated by

$$\omega_{c'/m} = \frac{\omega_c}{2}\left[1 \pm \sqrt{1 - 2\left(\frac{\omega_z}{\omega_c}\right)^2}\right], \tag{2}$$

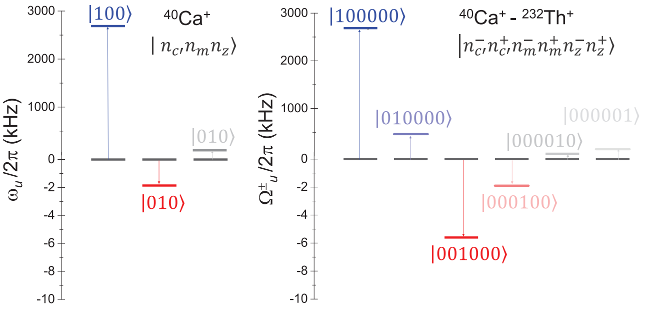

Fig. 1: Schematic representation of the eigenfrequency values and eigenvectors with respect to the ground state of motion for a single $^{40}Ca^{+}$ ion (left) and for an unbalanced ion crystal made of a $^{40}Ca^{+}$ and a $^{232}Th^{+}$ ion. The index u stands for c', m, and z.

where the subscripts c' and m stand for modified cyclotron and magnetron, respectively, and

$$\omega_c = \frac{q}{m}B. \tag{3}$$

From eq. (2), $\omega_c = \omega_{c'} + \omega_m$, although this only holds true for an ideal trap. All the experiments are subject to small misalignments and imperfections in the realization of the electric and the magnetic field, which becomes critical for high-precision experiments. Thus, due to its robustness [36], the relationship known as invariance theorem

$$\omega_c^2 = \omega_{c'}^2 + \omega_z^2 + \omega_m^2, \tag{4}$$

is rather used. Equation (4) has been generalized for an ion crystal made of two ions; one that can interact with laser beams, named sensor ion (s) with mass m_s and cyclotron frequency ω_{cs}, and the other to be studied, referred to as target ion (t) with mass m_t and cyclotron frequency ω_{ct}. The result of the generalization reads [37]

$$\omega_{cs}^2+\omega_{ct}^2 = (\Omega_{c'}^+)^2+(\Omega_{c'}^-)^2+(\Omega_m^+)^2+(\Omega_m^-)^2+(\Omega_z^+)^2+(\Omega_z^-)^2, \tag{5}$$

being $\Omega_{c'}^+$, $\Omega_{c'}^-$, Ω_m^+, Ω_m^-, Ω_z^+, and Ω_z^-, the modes' eigenfrequencies of the two-ion crystal formed by the sensor and target ions. The eigenfrequencies have been calculated numerically, using the linear approximation, for a large mass range $\mu = m_t/m_s$ considering singly charged ions [24]. These calculations have been extended to higher electronic charges in ref. [25]. Figure 1 depicts the eigenfrequencies of a single $^{40}Ca^{+}$ ion calculated from eqs. (1) and (2) (left) and those of a $^{40}Ca^{+}$-$^{232}Th^{+}$ ion crystal following the method described in refs. [24,25] (right). The quantum Hamiltonian of the crystal, up to the ground state energy, can be written in terms of creation and anhilation operators, as[1]

$$\begin{aligned} H = {} & \hbar\Omega_z^+ a_+^\dagger a_+ + \hbar\Omega_z^- a_-^\dagger a_- \\ & + \hbar\Omega_{c'}^+ b_{c',+}^\dagger b_{c',+} + \hbar\Omega_{c'}^- b_{c',-}^\dagger b_{c',-} \\ & - \hbar\Omega_m^+ b_{m,+}^\dagger b_{m,+} - \hbar\Omega_m^- b_{m,-}^\dagger b_{m,-}, \end{aligned} \tag{6}$$

[1]The derivation of eqs. (6), (7) and (8) is shown in the Supplementary Material `Supplementarymaterial.pdf` (SM).

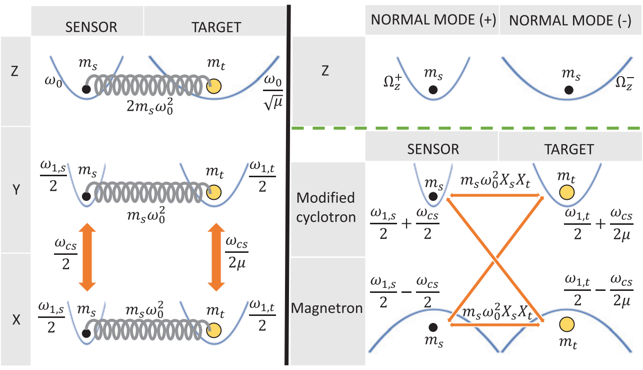

Fig. 2: Illustration of the normal mode diagonalization. Left: initial situation: one mode for each spatial dimension (z, y and x) and ion (sensor and target). Each ion's mode is coupled to its counterpart by a position-dependent force (spring shape). Additionally, modes x and y of each ion are coupled by a phonon-conserving interaction (orange arrows). Right: the z modes are diagonalized in a single step, providing normal modes $(+)$ and $(-)$. Modes x and y are diagonalized in two steps. First, the modified-cyclotron and magnetron modes are found for the target and sensor ions independently. This transforms the position-dependent force into an interaction that conserves the phonon number difference between both modified-cyclotron modes and magnetron modes (orange arrows). A final Bogolubov transformation V is necessary to fully diagonalize the system into the $+$ and $-$ modified-cyclotron and magnetron modes.

with the annihilation operator of the axial modes

$$a_{\pm} = \frac{1}{\sqrt{2\hbar}} \left(\sqrt{\frac{m_s \Omega_z^{\pm}}{2}} z_{\pm} + i \sqrt{\frac{2}{m_s \Omega_z^{\pm}}} p_{z,\pm} \right), \quad (7)$$

and the annihilation operators of the radial modes: modified-cyclotron normal modes $b_{c',+}$, $b_{c',-}$ and magnetron normal modes $b_{m,+}$, $b_{m,-}$.

These are the result of a diagonalization procedure that is illustrated in fig. 2, that we describe step by step in the SM and that we sketch in the following. The axial mode (z) requires a rescaling of the mass of the target ion to that of the sensor ion and a diagonalization of the resulting potential energy terms. The radial modes require a few more steps. First, we define the local annihilation operators, related to position and momentum operators of the ions through expressions

$$b_{k,t} = \frac{1}{\sqrt{2\hbar}} \left(\sqrt{\frac{m_t \omega_{1,t}}{2}} k_t + i \sqrt{\frac{2}{m_t \omega_{1,t}}} p_{k,t} \right),$$
$$b_{k,s} = \frac{1}{\sqrt{2\hbar}} \left(\sqrt{\frac{m_s \omega_{1,s}}{2}} k_s + i \sqrt{\frac{2}{m_s \omega_{1,s}}} p_{k,s} \right), \quad (8)$$

where k stands for either x or y and we define $\omega_{1,s} = \sqrt{\omega_{cs}^2 - 4\omega_z^2}$ and $\omega_{1,t} = \sqrt{\omega_{cs}^2/\mu^2 - 4\omega_z^2/\mu}$. Then, we define the unperturbed modified-cyclotron and magnetron modes by the two-mode transform $b_{c',r} = (b_{x,r} - i b_{y,r})/\sqrt{2}$ and $b_{m,r} = (b_{y,r} - i b_{x,r})/\sqrt{2}$, where r stands for either s or t. This transforms the initial position-dependent couplings between the sensor and target ions (fig. 2, left) into an interaction that conserves the phonon number difference between the unperturbed modified-cyclotron modes and the unperturbed magnetron modes (fig. 2, right). Finally, a Bogolubov transform produces the diagonal modes $b_{c',+}$, $b_{c',-}$, $b_{m,+}$ and $b_{m,-}$.

The representation in fig. 1 assumes that the single ion and the crystal are cooled to the ground state of motion and $n_{c'}^+$, $n_{c'}^-$, n_m^+, n_m^-, n_z^+, and n_z^- give the number of phonons with energies $\hbar\Omega_{c'}^+$, $\hbar\Omega_{c'}^-$, $\hbar\Omega_m^+$, $\hbar\Omega_m^-$, $\hbar\Omega_z^+$, and $\hbar\Omega_z^-$, respectively. In order to reach the ground state of motion for a single ion in the Penning trap ($\langle n_u^{\pm} \rangle = 0$), two procedures can be followed sequentially: Doppler and sideband cooling [28]. The technique described here will use $^{40}Ca^+$ as sensor ion, and its electronic transitions at $\lambda \sim 397$ nm (electric dipole) and $\lambda \sim 729$ nm (dipole forbidden), respectively, for Doppler and sideband cooling. While the axial motion in a Penning trap can be treated analogously to the axial motion in a linear radiofrequency trap [38], cooling the radial motion differs due to the unstable magnetron motion. So far, the group at Imperial College has reported $\langle n_{c'} \rangle = 0.35(5)$, and $\langle n_m \rangle = 1.7(2)$ after performing sideband cooling of a single $^{40}Ca^+$ ion in a 1.89 tesla Penning trap [28]. In the experiment in Granada, the $^{40}Ca^+$ ion is stored in a 7 tesla Penning trap. The higher intensity has made Doppler cooling more challenging, therefore requesting a more complex laser system [23,25]. The radial eigenfrequencies (eq. (2)), can be tuned by adjustment of the U due to their dependency on the frequency ω_z apparent in eq. (1). Throughout this publication $\omega_z = 2\pi \times 100\,\text{kHz}$, which yields $\omega_m = 2\pi \times 1.86\,\text{kHz}$ and $\omega_{c'} = 2\pi \times 2.6875\,\text{MHz}$ (fig. 1). While $\omega_{c'}$ is a factor of about 4 larger than the value quoted in ref. [28], ω_m is a factor of ~ 28 smaller, and this might prevent the proper cooling of the magnetron motion. The potential U can be tuned so that $\omega_z = 2\pi \times 500\,\text{kHz}$, resulting in ω_m approximately the same as in ref. [28], while maintaining a large value of $\omega_{c'}$ ($2\pi \times 2.6421\,\text{MHz}$). For this configuration, the distance between the two laser-cooled ions in the crystal is $\sim 9\,\mu$m and they can be resolved with the optical system. Cooling the magnetron motion is a pre-requisite for Quantum Mass Spectrometry, since a number of phonons in either of the magnetron modes shifts $\Omega_{c'}^-$, the frequency requiring the highest accuracy, by more than 100 mHz [24,25]. The full crystal may be cooled due to the Coulomb interaction between the $^{40}Ca^+$ and the ion under study. Note that the choice of $^{232}Th^+$ (fig. 1) is motivated by a project in the laboratory.

Motional quantum metrology on a two-ion crystal. – The eigenfrequencies of a single ion are probed by external fields so as to get ω_c from eq. (4). In the case of an ion crystal, the quantity to be determined is the cyclotron frequency of the target ion ω_{ct}, and for this goal ω_{cs}

and the six eigenfrequencies of the crystal (eq. (5)) are independently measured. The eigenfrequency that requires the most accuracy is, as mentioned above, $\Omega_{c'}^{-}$ (fig. 1). The method for these measurements is based on the one described in ref. [27] for a single $^{25}\mathrm{Mg}^{+}$ ion. The perturbation due to an external, oscillating dipolar field produces a displacement in mode a of the form

$$\hat{D}(\alpha) = e^{\alpha\hat{a}^{\dagger} - \alpha^{*}\hat{a}}, \tag{9}$$

with a displacement amplitude α related to the strength of the electric field E, the detuning δ between its oscillating angular frequency and that of the mode, the initial phase of the oscillating field θ, the ground state extension of the mode z and the time t_D the oscillating field is applied by

$$\alpha = \frac{qEz}{2\hbar} e^{i(\delta\cdot t_D + \theta)} \times t_D. \tag{10}$$

This can be generalized for the case of an unbalanced crystal since the six eigenmodes are decoupled, and the production of coherent states can be resonantly selected. It is necessary to compute the displacement amplitude α_k associated to each of the six modes k

$$\alpha_k = \frac{qE_k\xi_k}{2\hbar} e^{i(\delta_k\cdot t_D + \theta)} \times t_D, \tag{11}$$

where each mode will see a different projection of the electric field E_k, a different detuning δ_k and will be characterized by a different characteristic coordinate ξ_k. In order to accommodate the phases originating in the Bogolubov transforms, both E_k and ξ_k are understood as complex numbers for radial modes.

We consider a uniform (but time-dependent) electric field with components in all axes $\mathbf{E}(t) = \cos(2\pi\nu_D t)(E_x\mathbf{i} + E_y\mathbf{j} + E_z\mathbf{k})$. Since the motions in the axial direction and radial plane are decoupled in the Penning trap, the effect of the field on them can be also treated separately.

Both axial modes see the same electric field intensity $E_{z,\pm} = E_z$, and have different characteristic coordinates

$$\xi_{z,\pm} = c_{\pm} Z_{\pm}, \tag{12}$$

with $Z_{\pm} = \sqrt{\hbar/(2m_s\Omega_z^{\pm})}$ and $c_{\pm} = c_s^{\pm} + c_t^{\pm}/\sqrt{\mu}$, where $c_s^{\pm}$ and $c_t^{\pm}$ are coefficients that can be understood as the components of the unitary matrix diagonalizing the matrix of the axial potential energy.

For radial modes, we must distinguish the electric field seen by the modified-cyclotron modes $E_{c',\pm} = (E_x - iE_y)/\sqrt{2}$ and by the magnetron modes $E_{m,\pm} = E_{c',\pm}^{*}$. Regarding the characteristic coordinates

$$\xi_{c',\pm} = X_s\left(u_{c',\pm}^{s} - iv_{c',\pm}^{s}\right) + X_t\left(u_{c',\pm}^{t} - iv_{c',\pm}^{t}\right), \tag{13}$$

$$\xi_{m,\pm} = -X_s\left(u_{m,\pm}^{s} + iv_{m,\pm}^{s}\right) - X_t\left(u_{m,\pm}^{t} + iv_{m,\pm}^{t}\right), \tag{14}$$

where $X_t = \sqrt{\hbar/m_t\omega_{1,t}}$ and $X_s = \sqrt{\hbar/m_s\omega_{1,s}}$ and u_k^j, v_k^j are components of the Bogolubov transformation matrix V diagonalizing the radial Hamiltonian[2].

[2]The Bogolubov transformation matrix V is shown in the SM.

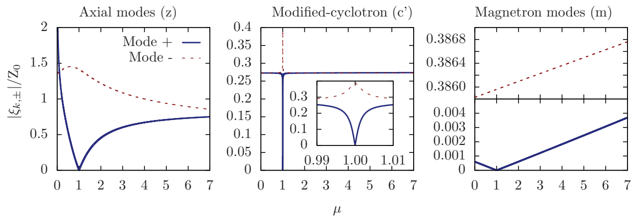

Fig. 3: Absolute values of the characteristic coordinates $|\xi_{k,\pm}|$ for $k \in \{z, c', m\}$ as a function of μ and in units of $Z_0 = \sqrt{\hbar/(2m_s\omega_z)}$. In this calculation, $\omega_z/\omega_c = 0.03719$.

All characteristic lengths are plotted in fig. 3 as a function of μ and for a trap characteristic $\omega_z/\omega_{cs} = 0.03719$. All of them are expressed in units of the axial ground state extension of the sensor ion in isolation $Z_0 = \sqrt{\hbar/(2m_s\omega_z)}$. For balanced crystals ($\mu = 1$) the dipolar field only couples to the center of mass mode ($-$). Otherwise, all modes can be addressed, albeit the magnetron ($+$) mode features the weakest coupling to the dipolar field, thus requiring electric fields stronger by even a couple orders of magnitude for similar accuracies.

The read out process consists in mapping the overlap between the initial ground state and the displaced states ($\langle 0|\hat{D}(\alpha)|0\rangle^2$) through the encoded qubit formed by the $^2\mathrm{S}_{1/2}$ ($|\downarrow\rangle$) and $^2\mathrm{D}_{5/2}$ ($|\uparrow\rangle$) states in $^{40}\mathrm{Ca}^{+}$ using RAP, *i.e.*, by applying a frequency-chirped pulse with Gaussian envelope centered first at the carrier frequency and then at the first blue sideband (BSB). RAP has been performed on $^{40}\mathrm{Ca}^{+}$ using the transition $^2\mathrm{S}_{1/2} \rightarrow {}^2\mathrm{D}_{5/2}$ [29,30]. The population in the ground state ($|0000000;\downarrow\rangle$) can be determined using the $^2\mathrm{S}_{1/2} \rightarrow {}^2\mathrm{P}_{1/2}$ transition, by observing the 397 nm photons. This is done for several frequency values of the field applied, in order to build a resonance curve around each of the mode's frequency. The time needed for the measurement depends on t_D, the evolution time of the system T, which produces an accumulated phase $\Phi = \delta \times T$, and on the time for state read out. This is done for different oscillations frequencies of the electric field around that of the mode to be driven. The final uncertainty in the standard quantum limit depends on T, t_D, the number of measurements N, and $|\alpha_k|$ [27].

The apparatus and experimental results. – Motional quantum metrology proposed in this manuscript will be carried out with the open-ring Penning trap of the TRAPSENSOR facility [23,25]. The center of the trap is located in a highly homogeneous region of a magnetic field with an intensity of 7 tesla provided by a superconducting solenoid ($\Delta B = 0.1$ ppm in a volume of 1 cm^3). Figure 4 shows a three-dimensional CAD drawing of the trap (left) and a longitudinal cut (right). Calcium ions are produced inside the Penning trap [23], or outside the superconducting solenoid in an open-ring Paul trap [39]. The calcium atoms are released in both systems by heating a commercial atomic oven, placed with a certain orientation around the trap volume. The evaporated atoms interact with two

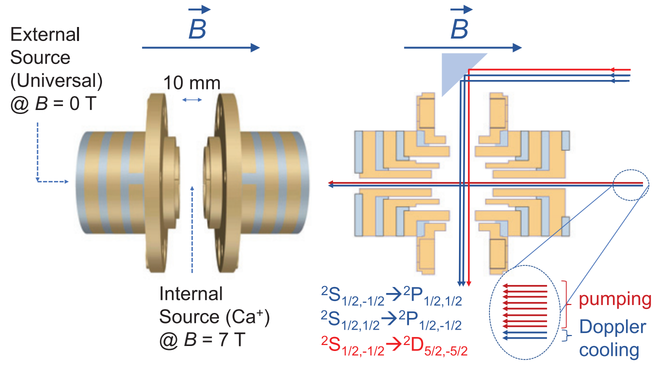

Fig. 4: CAD drawings of the open-ring Penning trap: three-dimensional drawing (left) and longitudinal cut (right). The color gold/orange indicates the electrodes while grey/blue is used for the insulators. See text for further details.

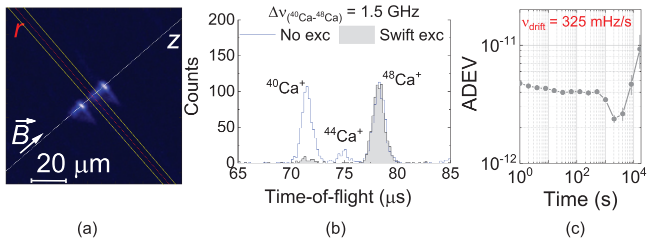

Fig. 5: Some pictures summarizing the status of the experiment and what has been reached so far: (a) image of a balanced crystal ($^{40}Ca^+$-$^{40}Ca^+$) in the open-ring Penning trap obtained with an electron multipliying charge-coupled device (EMCCD) [39]. (b) Time-of-flight (tof) spectrum showing ions from different calcium isotopes, ejected from the Penning trap and recorded with a micro-channel plate (MCP) detector (blue solid line). Also shown is the tof spectrum of $^{48}Ca^+$ ions (grey-shaded area) when removing the other isotopes using the stored waveform inverse Fourier transform (SWIFT) technique [41]. (c) Allan deviation (ADEV) from a frequency comb measurement of the laser frequency locked to a high-finesse cavity to drive the dipole-forbidden transition $4s^2S_{1/2,-1/2} \rightarrow 3d^2D_{5/2,-5/2}$. The frequency drift as a function of the time is 325 mHz/s in 30 hours of measurement [42].

laser beams, one tunable to drive the transition $^0S_0 \rightarrow {}^1P_1$ of the calcium atom ($\lambda \sim 423$ nm) and the other one at a fixed wavelength ($\lambda = 375$ nm) to move the excited electron to the continuum. By tuning the frequency of the first laser, it is possible to select any of the calcium isotopes present in the sample. When the ions are produced inside the Paul trap, they have to be ejected, transported and captured in the Penning trap. Using the two production schemes, Doppler cooling has been performed on ion clouds, forming balanced crystals and reaching the single ion sensitivity [39]. This requires ten different laser frequencies tuned with an absolute accuracy of 10 MHz, compared to just the two values needed in the absence of a strong magnetic field [23]. Due to the high intensity of the field, the non-degenerate $^2P_{1/2,m_{1/2}}$ and $^2D_{5/2,m_{5/2}}$ states are mixed [40].

The right part of fig. 4 shows schematically twelve laser beams (to cool the ions in the axial and radial direction). The transitions $^2S_{1/2,\pm1/2} \rightarrow {}^2P_{1/2,\mp1/2}$ for cooling and read out, and the transition $^2S_{1/2,-1/2} \rightarrow {}^2D_{5/2,-5/2}$ to generate and manipulate the quantum bit from the coherent state to other configurations, are shown. Note that the qubit transition is not optimal for the axial modes but it might work out assuming the angle between laser beam and magnetic field is slightly deviated from 90 degrees. The laser frequency values have been summarized in ref. [23] and the calculations presented in detail in ref. [25]. The status of the experiment is briefly summarized in fig. 5:

a) EMCCD image of the collimated 397 nm photons from two ions forming a crystal along the magnetic-field axis of the Penning trap. In this measurement, the ions were created inside the Penning trap. In this case $\omega_z \approx 2\pi \times 170$ kHz, implying for the balanced crystal, a distance between the centers of the projections of the photons distributions along the $\mathbf{B}$ line of about 18 μm. The distance of 9 μm ($\Omega_z^- = 2\pi \times 500$ kHz) is also indicated in the figure (yellow dotted lines). A photomultiplier tube has been also installed together with the EMCCD, allowing recording high signal-to-noise ratios for a single trapped ion within acquisition times in the order of milliseconds. A full and detailed description of this setup and measurements is given in ref. [39].

b) Time-of-flight spectrum showing different calcium isotopes produced inside the Penning trap and ejected towards an MCP detector. The photoionization laser was tuned to be in resonance with the $^0S_0 \rightarrow {}^1P_1$ transition in ^{48}Ca. Due to its low natural abundance (0.187%) compared to that of $^{40}Ca^+$ (96.941%), the latter is observed in the spectrum with the same intensity as $^{48}Ca^+$. Such a configuration anticipates that it will be possible to form an unbalanced $^{48}Ca^+$-$^{40}Ca^+$ ion crystal prior to the $^{232}Th^+$-$^{40}Ca^+$ one, to carry out a proof of principle experiment. A mini radiofrequency quadrupole (RFQ) structure [43] built by the group of Michael Block, is currently under commissioning in the beamline to produce and inject $^{232}Th^+$ ions in the Penning trap. Besides thorium ions, the mini-RFQ will allow injecting other ion species produced from metallic samples by laser ablation (for laser ablation see, *e.g.*, [44]).

c) Allan deviation from a 30 hours measurement of the laser frequency generated by a tunable diode laser locked to a high-finesse temperature-stabilized cavity, to drive the qubit transition in $^{40}Ca^+$. The frequency was measured by means of a frequency comb [42]. The frequency drift *vs.* time is 325 mHz/s. The implementation of the acoustic optical modulators (AOMs) required to match the frequency of the laser beam after the cavity to that of the transition $^2S_{1/2,-1/2} \rightarrow {}^2D_{5/2,-5/2}$ is under way and will be firstly tested in a linear Paul trap. Such AOM will also allow shaping the frequency-chirped pulse for RAP. A transition with $\Delta m_j = \pm 1$ that might be used for the axial modes can be also tested.

The results shown in fig. 5 certify a significant progress in the experiment. Two PhD Theses (by Joaquín Berrocal and Francisco Domínguez) are devoted to bringing the experiment to the situation presented here and to optimize it to meet the requirements for the proposed experiment.

Conclusions and perspectives with the Penning trap platform. – In this publication, we have developed the concept of motional quantum metrology to measure motional frequencies of a two-ion crystal cooled to its ground-state of motion in a Penning trap. Such a platform is universal as it will always use the same qubit, the $^2S_{1/2}$ ($|\downarrow\rangle$) and $^2D_{5/2}$ ($|\uparrow\rangle$) states in $^{40}Ca^+$, to measure the modes' frequencies of the crystal. The facility around the open-ring Penning trap [23] is at the stage to carry out the first proof of principle experiment in the short-term future. Balanced ion crystals have already been produced using ions generated with an external ion source [39], a precursor to the formation of hybrid crystals. The performance of the 729 nm laser locked to the high-finesse cavity to drive the qubit transition meets the requirements [42]. The only remaining issue is to match the frequency of the system to that of the transition, as the free spectral range of the cavity is about 1.5 GHz. This is done by means of two AOMs. The three eigenfrequencies of a single $^{40}Ca^+$ ion needed to obtain ω_{cs} can be measured utilizing the same scheme as for the crystal. Such a procedure will allow obtaining measurements with uncertainties below the standard quantum limit.

Besides the proposed motional quantum metrology experiment, the two-ion crystal in the existing Penning trap can be utilized to perform precision spectroscopy on any target ion, taking the advantage of cooling it through the sensor ion or implementing schemes and procedures such as quantum logic [26] for accurate measurements of the frequencies of narrow-linewidth transitions, although now in the absence of RF fields. The ^{232}Th atom for example, has been investigated in several electronic charge states with the motivation to make experiments on the low-lying isomer ^{229m}Th, proposed as the only candidate to build a nuclear clock [31,32] (see also the recent review [45]). $^{232}Th^{3+}$ and $^{229}Th^{3+}$ ions have been laser-cooled in a Paul trap [46,47]. Spectroscopy (without laser cooling) on the 402 nm transition on $^{232}Th^+$ has also been carried out in a Paul trap using one- and two-photon laser excitation [48]. A recent experiment has also been reported on sympathetic cooling of $^{232}Th^+$ via laser-cooled $^{40}Ca^+$ ions in a linear Paul trap [33]. In our Penning trap $^{40}Ca^+$-$^{232}Th^+$ configuration in the 7 tesla magnetic field, the transitions in $^{232}Th^+$ can be probed after cooling to the ground state through the $^{40}Ca^+$ ion, and the same can be done with any ion from other thorium isotope delivered by the source regardless of its charge state. The magnetic field will break state degeneracy and this might also allow for measurements of the electronic g_J-factors. Although the production of ^{229m}Th ions is cumbersome [49], the confinement of a ^{229m}Th ion will not differ from that of $^{232}Th^+$ and the nuclear transition from the isomeric to the ground state (at $\lambda \sim 150\,\text{nm}$) can be studied once the crystal is formed. Note that the ^{229m}Th atom has a nuclear spin $I = 3/2$, that shifts the frequency of the transition by up to $\nu = g_N \mu_N/(hB)$, where g_N is the nuclear g-factor (which can be measured for the particular case of ^{229m}Th), μ_N is the nuclear magneton and h the Planck's constant. ^{229m}Th has to be produced and handled in dedicated facilities.

Another interesting case which can be handled with the Penning-trap platform using a laser ablation ion source is the $^{139}La^{2+}$ ion, the hyperfine structure of which has been studied [34] and a system for trapping and cooling is under completion [50]. The transitions of interest for this ion are the $^2D_{3/2} \rightarrow {}^2F_{5/2}$ and $^2D_{5/2} \rightarrow {}^2F_{7/2}$ with $\lambda \sim 1390$ and $\sim 1410\,\text{nm}$, respectively, which can be accessed taking advantage of the available technology in the telecom regime. In the Penning trap described here, the $^{40}Ca^+$-$^{139}La^{2+}$ crystal can be formed in the same way as the $^{40}Ca^+$-$^{232}Th^{1+}$ one by exchanging the thorium by a lanthanum target. Thus, different experiments can utilize the same qubit for readout. For spectroscopy, although the high-intensity of the magnetic field will produce many transitions, they can be driven or read using electro-optical modulators.

* * *

DR acknowledges support from the Spanish MCINN through the project PID2019-104093GB-I00/AEI/10.01339/501100011033, and from the Andalussian Government through the project P18-FR-3432. DR warmly thanks all collaborators and co-workers since the activity started, specially the two PhD students who are working daily on the experiments in the Ion Traps and Lasers Laboratory: Francisco Domínguez and Joaquín Berrocal. The construction of the facility was supported by the European Research Council (contract No. 278648-TRAPSENSOR), projects FPA2015-67694-P and FPA2012-32076, infrastructure projects UNGR10-1E-501, UNGR13-1E-1830 and EQC2018-005130-P (MICINN/FEDER/UGR), and IE-5713 and IE2017-5513 (Junta de Andalucía-FEDER). JC acknowledges support from *Ministerio de Ciencia, Innovación y Universidades* (Spain) ("Beatriz Galindo" Fellowship BEAGAL18/00081).

Data availability statement: The data that support the findings of this study are available upon reasonable request from the authors.

REFERENCES

[1] Brown L. S. and Gabrielse G., *Rev. Mod. Phys.*, **58** (1986) 233.

[2] Gabrielse G. *et al.*, *Phys. Rev. Lett.*, **82** (1999) 3198.
[3] Wineland D. J. and Dehmelt H. G., *J. Appl. Phys.*, **46** (1975) 919.
[4] Sturm S. *et al.*, *Nature*, **506** (2014) 467.
[5] Ulmer S. *et al.*, *Nature*, **524** (2015) 196.
[6] Cornell E. A. *et al.*, *Phys. Rev. A*, **45** (1992) 3049.
[7] Bradley M. P. *et al.*, *Phys. Rev. Lett.*, **83** (1999) 4510.
[8] Rainville S. *et al.*, *Science*, **303** (2004) 334.
[9] Myers E. G., *Atoms*, **37** (2019) 1.
[10] Ulmer S. *et al.*, *Rev. Sci. Instrum.*, **80** (2009) 123302.
[11] Vogel M. *et al.*, *Phys. Rev. A*, **90** (2014) 043412.
[12] Micke P. *et al.*, *Rev. Sci. Instrum.*, **89** (2018) 063109.
[13] Rodríguez D., *Appl. Phys. B*, **107** (2012) 1031.
[14] Heinzen D. J. and Wineland D. J., *Phys. Rev. A*, **42** (1990) 2977.
[15] König M. *et al.*, *Int. J. Mass Spectrom. Ion Process.*, **142** (1995) 95.
[16] Block M. *et al.*, *Nature*, **463** (2010) 785.
[17] Minaya Ramirez E. *et al.*, *Science*, **337** (2012) 1207.
[18] Eliseev S. *et al.*, *Phys. Rev. Lett.*, **110** (2013) 082501.
[19] Giacoppo F. *et al.*, in preparation (2021).
[20] Lohse S. *et al.*, *Rev. Sci. Instrum.*, **90** (2019) 063202.
[21] Lohse S. *et al.*, *Rev. Sci. Instrum.*, **91** (2020) 093202.
[22] Berrocal J. *et al.*, *Quantum Sci. Technol.*, **6** (2021) 044002.
[23] Gutiérrez M. J. *et al.*, *New J. Phys.*, **21** (2019) 023023.
[24] Gutiérrez M. J. *et al.*, *Phys. Rev. A*, **100** (2019) 063415.
[25] Gutiérrez M., *Studying an unbalanced two-ion crystal in a Penning trap: towards the quantum regime in high magnetic field*, PhD Thesis, Universidad de Granada (2021).
[26] Schmidt P. O. *et al.*, *Science*, **309** (2005) 749.
[27] Wolf F. *et al.*, *Nat. Commun.*, **10** (2019) 2929.
[28] Hrmo P. *et al.*, *Phys. Rev. A*, **100** (2019) 043414.
[29] Wünderlich C. *et al.*, *J. Mod. Opt.*, **54** (2007) 1541.
[30] Watanabe T. *et al.*, *Phys. Rev. A*, **90** (2011) 033412.
[31] Peik E. and Tamn C., *Europhys. Lett.*, **61** (2003) 181.
[32] Campbell C. J. *et al.*, *Phys. Rev. Lett.*, **108** (2012) 120802.
[33] Groot-Berning K. *et al.*, *Phys. Rev. A*, **99** (2019) 023420.
[34] Olmschenk S. *et al.*, *Phys. Rev. A*, **96** (2017) 032502.
[35] Patterson D., *Phys. Rev. A*, **97** (2018) 033403.
[36] Brown L. S. and Gabrielse G., *Phys. Rev. A*, **25** (1982) 2423.
[37] Jain S. *et al.*, *Phys. Rev. X*, **10** (2020) 031027.
[38] Leibfried D. *et al.*, *Rev. Mod. Phys.*, **75** (2003) 281.
[39] Berrocal J. *et al.*, in preparation (2021).
[40] Crick D. R. *et al.*, *Phys. Rev. A*, **81** (2010) 052503.
[41] Guan S. and Marshall A. G., *Int. J. Mass Spectrom. Ion Process.*, **157-158** (1996) 5.
[42] Domínguez F. *et al.*, in preparation (2021).
[43] Andelic B. *et al.*, *Hyperfine Interact.*, **241** (2020) 46.
[44] Cornejo J. *et al.*, *Nucl. Instrum. Methods B*, **317** (2013) 522.
[45] Peik E. *et al.*, *Quantum Sci. Technol.*, **6** (2021) 034002.
[46] Campbell C. J. *et al.*, *Phys. Rev. Lett.*, **102** (2009) 233004.
[47] Campbell C. J. *et al.*, *Phys. Rev. Lett.*, **106** (2011) 223001.
[48] Herrera-Sancho O. A. *et al.*, *Phys. Rev. A*, **85** (2012) 033402.
[49] von der Wense L. *et al.*, *Nature*, **533** (2019) 47.
[50] Olmschenk S., private communication.